A Novel Ultra-Miniaturized THz Refractive Index-Based Material Sensor

Anbuselvi Mathivanan
SSN College of Engineering: Sri Sivasubramaniya Nadar College of Engineering
Aruna Veeraselvam (arunav@ssn.edu.in)
SSN College of Engineering: Sri Sivasubramaniya Nadar College of Engineering https://orcid.org/0000-0002-5519-3933
Gulam Nabi Alsath Mohammed
SSN College of Engineering: Sri Sivasubramaniya Nadar College of Engineering

Research Article

Keywords: THz Sensors, Metamaterials, Single-band, Highly sensitive

Posted Date: March 14th, 2022

DOI: https://doi.org/10.21203/rs.3.rs-1341690/v1

Abstract

This paper discusses the design, characterization and analysis of an ultra-miniaturized and highly sensitive metamaterial THz sensor for material sense. A novel spin-shaped resonator integrated with hexagonal is designed as an absorber to perform material sensing operations. The footprint of the proposed sensor is $0.67\lambda eff \times 0.67\lambda_{eff}$ where λ_{eff} is the effective wavelength calculated at 7.16 THz. The proposed THz sensor is analyzed based on the absorption characteristics by estimating the sensitivity of the metamaterial sensor. The proposed sensor offers 99.9% absorptivity under free-space conditions. The proposed THz sensor exhibits rotational symmetry and hence it is insensitive to polarization changes. Furthermore, the proposed sensor is angularly stable for oblique incidences up to 60˚. The sensor performance is estimated for different refractive indices of various analytes and the average sensitivity is estimated as 1.37 THz/Refractive Index Unit (RIU). The impact of the thickness of the analyte is analyzed and the average deviation of 59 GHz/μm is reported. Thus, it is concluded that the proposed metamaterial THz sensor is best suitable for different material sensing applications.

I. Introduction

Recently researchers are attracted to the investigations using the Terahertz (THz) radiation for its non-invasive characteristics and thus the radiation non-ionizes the human body. The THz occupies the electromagnetic spectrum in the range between 0.1 THz to 10 THz. This spectrum range is suitable for better surface penetration capability with lesser energy consumption. These THz waves are widely investigated and applied in different domains viz. communication [1], spectroscopy [2], imaging [3], sensing [4], and material characterization [5]. In the recent world, researchers use metamaterials for designing the miniaturized THz components and devices. The metamaterial is an artificially engineered material that has unique properties like tunable negative permittivity, permeability [6–7], and refractive index properties which are difficult in natural materials. These exclusive properties are mainly used in the development of resonant components with minimum loss such as sensors and absorbers. The sensors and absorbers are applied for different areas of material characterization, sensing of biomedical components, etc. These metamaterial sensors can absorb strong electromagnetic radiation [8]. Thus, this research is focused on designing a metamaterial THz sensor for material characterization.

In general, the sensor performance is validated based on the absorption characteristics by focusing the THz radiation on the sensor. The resonant characteristic is allowed to vary by either red or blue shift in the absorption peak while the THz sensor is loaded with the analyte. The transmission, reflection, and absorption coefficients are considered for estimating the characteristics of the sensor. Amidst this, the absorption coefficient is primarily considered for estimating the absorptivity of the sensor which validates the sensing performance.

In literature, various studies on THz sensors for material characterization are reported. In [9], Landy et. al. has initiated a perfect metamaterial sensor using a split ring resonator. The authors in [10] have designed an electric ring resonator with an absorptivity of 99.6% at the operating frequency of 0.84 THz. Later, the

same work as in [10] is extended for attaining polarization stability with its equivalent circuit is reported in [11]. In [12], the authors have proposed an ultra-sensitive double F-shaped resonator whose footprint is 1.029λeff × 1.209λeff which operates at 5.92 THz with the absorptivity of 95% for biomedical application. In [13], a biomedical sensor is designed using a split-ring resonator with the size 0.391λeff × 0.391λeff which resonates at 2.249THz with 300 GHz/RIU as sensitivity. The significance of high resonance is discussed in [14], where a split ring resonator is designed to support high resonance at 1.5 THz with FWHM as 514 GHz. The authors in [15] have proposed a near-field sensor using metamaterial based on a subwavelength regime. The size of the sensor in [15] is 0.763λeff × 0.763λeff, with the sensitivity as 430 GHz/RIU at 1.52 THz. In [16], a label-free sensor is designed using a circular hole array with a footprint of 1.368λeff × 1.368λeff resonates at 0.557 THz has a sensitivity of 128 THz. A multi-band metamaterial absorber of size 1.317λeff × 1.317λeff is proposed in [17], which resonates at 0.22 THz, 0.48 THz, 0.72 THz, and 0.76 THz with an average absorptivity of 75% and sensitivity of 139.2 GHz/RIU for various refractive indexes. Similarly, the multiband material absorber is reported in [18], which resonates at 4.682 THz, 5.150THz, 5.310THz and 5.814THz with 99.6% of average absorptivity and refractive index sensitivity of 0.471 THz/RIU. In [19], the authors have proposed a quadband absorber for biomedical application with the highest sensitivity of 423 GHz/RIU. The researchers in [20], reported a flexible metamaterial THz sensor whose footprint is $0.326\lambda_{eff} \times 0.326\lambda_{eff}$. The proposed sensor in [20] discusses the stability analysis for a wide angle of incidence with the absorptivity of 97% at 1.6 THz. The authors in [21] have used superconductive metamaterial to study intensity and phase modulation. In [22], a plasmonic refractive index sensor is designed and dispersion characteristics are examined. The research is extended to design a dual-band absorber in the optical regime as in [23]. Thus, the study on various metamaterial THz sensors provides a wide area to propose a novel metamaterial THz unit cell for sensing the materials in different applications using their refraction index.

In this research, a metamaterial THz sensor is reported for material sensing applications. The proposed highly sensitive, the ultra-miniaturized sensor has a unit cell which is a subwavelength element for constructing a near-infinite periodic array. This organization of the paper is as follows: The design of the sensor and its characterization are discussed in the second section. The third section consists of an analysis of polarization and angular stability. The analysis of the sensing performance of the designed THz sensor is discussed in the fourth section and finally, the conclusion is given in the last section.

II. THz Sensor Design

The design and analysis of the highly sensitive metamaterial THz sensor for material characterization based on the refractive index is discussed in this section. This research uses Surface Plasmon Resonance (SPR) as the optical sensing technique. This technique offers high quality of data and high throughput with the help of a lesser quantity of the analyte. Thus, it also offers good repeatability, reproducibility, the limit of detection, and best suits for real-time sensing [24–25]. Therefore, the THz sensor is designed for high sensitivity which operates at 7.16 THz with 99.9% absorptivity.

A. Construction

The construction of the proposed metamaterial THz sensor is shown in Fig. 1. A spinner enclosed in a hexagon is designed on the THz sensor as the top conducting layer is shown in Fig. 1a. The perspective view and side view of the proposed highly sensitive terahertz sensor is shown in Fig. 1b and Fig. 1c respectively. The overall size of the proposed THz sensor is 15 (L) μm x 15 (W) μm. Gold is used as the conducting layer whose frequency-dependent electrical conductivity is 4.56×10^{7} S/m. The designed structure is placed over the lossy polyimide substrate whose dielectric constant is 3.5 and the loss tangent is 0.0027 at 7.16 THz. Furthermore, polytetrafluoroethylene (Teflon) provides the mechanical support which is placed beneath the polyimide substrate and above the ground as depicted in Fig. 1b. The optimized dimensions of the proposed metamaterial THz sensor for achieving the highest absorption peak and sensitivity are shown in Table I. In CST microwave studio 2018, the Particle Swarm Optimization (PSO) technique is used for the optimization of the geometrical parameters with the count of mesh lines to be 10 per wavelength along with 10^{-6} as accuracy in the frequency domain solver (FDS) of the full-wave EM solver to meet the real-time performance. The thickness of the gold layer (h3) is 20 nm which is optimized between the range of values from 40nm to 10nm to obtain the peak absorptivity. As the thickness of conducting layer increased to 40nm, the resonant frequency blue shifts with the same level of absorptivity. Similarly, the reduced thickness causes a red shift in frequency with a lesser absorptivity of 99%. The characteristics such as transmission (T), reflection (R), and absorption (A) are analyzed using the finite integration technique (FIT) in CST. Along with that, the periodic boundary conditions are set along ‘x’ and ‘y’ directions, and the excitation is applied on z-direction using Floquet mode theory for the analysis. Similarly, the subwavelength elements [26–28] are analyzed using the Floquet mode theory. Once excited, the scattering parameters are used to derive the absorption characteristic of the designed metamaterial THz sensor. The absorptivity is estimated using Eq. (1).

$$A = 1 - |\Gamma_r|^2 - |\Gamma_t|^2 = 1 - |S_{11}|^2 - |S_{21}|^2 \quad (1)$$

$|\Gamma_t| = 0$ prevents the THz wave on the rear side of the sensor due to the placement of metamaterial below the substrate. Thus, Eq. (1) is reduced to Eq. (2)

$$A = 1 - |\Gamma_r|^2 = 1 - |S_{11}|^2 \quad (2)$$

TABLE I GEOMETRICAL DIMENSIONS OF THE DESIGNED THZ SENSOR

Parameters	L	W	L1	L2	L3	W1	W2	W3
Value (μm)	15	15	4. 81	2.37	5.5	0.1	0.1	0.2
Parameters	a	b	c	d	h	h1	h2	h3
Value (μm)	1.15	2.4	1.85	0.1	0.02	8	1	0.02

B. Evolution

Figure 2 shows the different stages of the evolution of spin structured THz. The absorption characteristics of each stage of evolution are shown in Fig. 3. The structure initiates with the interconnected triple outward arrow as shown in Fig. 2a with the thickness of pole as 0.1 μm and arrow as 0.02 μm. The proposed THz sensor resonates at 7.57 THz with 99% of absorption as shown in Fig. 3. Further to increase the absorptivity, three inward arrows are inserted at the intersecting points in the previous stage as depicted in Fig. 2b. As the inductance of the design is improved, the sensor resonates at the same frequency with increased absorption of 99.8%. Then, the electrical length is increased by connecting the inward and outward arrows and enclosed in a hexagon of width 0.2 μm to lower the resonant frequency as shown in Fig. 2c. Thus, the designed sensor has an absorptivity of 99.9% at 7.16 THz as shown in Fig. 3.

The proposed THz sensor is characterized using three spectra viz. the reflection, absorption and transmission as depicted in Fig. 4. It is inferred from the figure, that the proposed THz sensor shows very low reflection characteristics and zero transmission. Thus, the sensor shows high absorptivity at 7.16 THz. It is better to confirm the accuracy of the simulation by simulating the designs reported in [13] and [20]. During the simulation, the software retains the setup which is used for the sensor presented in this work. The count of mesh lines per wavelength is fixed to 15 and the accuracy as 10^{-6} is fixed in the frequency domain solver of the full-wave EM solver. This results in the absorption characteristics as in [13] and [20]. Thus, it is confirmed that the designed THz sensor if fabricated and measured, will provide a good result as described in [20].

C. Surface plasmon effects

The Surface Plasmon Wave (SPW) refers to the oscillations of charge density at the interface between the metal and dielectric at the resonant frequency [29–30]. Thus, the high concentration of surface plasmon is confined at the interface. This surface plasmon mode depends on the refractive index of the dielectric material [31]. Therefore, the distribution of electric field over the proposed metamaterial THz sensor is analyzed at 7.16 THz is shown in Fig. 5. It is observed from Fig. 5, that a high density of surface plasmon is present on the arms of the spin-shaped resonator and also on the vertical arms of the hexagon ring. Similarly, the least plasmon density can be seen on the upper part of the hexagon ring and on the conductor connecting the spin and hexagon as depicted in Fig. 5.

D. Influence of conductors

The absorption characteristics of the designed metamaterial THz sensor for the other two conductors are analyzed and depicted in Fig. 6. The frequency-independent Gold is used as the conducting material in the proposed spin-shaped THz sensor whose conductivity is 4.56×10^7 S/m. The absorption characteristics of other materials like copper and platinum are observed whose conductivities are 5.8×10^7 S/m and 9.52×10^6 S/m, respectively, which are frequency-independent.

It is inferred from the figure, that the absorptivity is reduced with a redshift in resonant frequency for Platinum due to reduced conductivity. Since Platinum is a noble metal, the plasma frequency is

proportional to the material conductivity. Henceforth, Platinum shows inferior absorption characteristics compared to Copper and Gold. Since the oscillations of plasmon on the resonator surface depend on the used material conductivity, Copper and Gold shows similar performance as the conductivity is nearly matched and the shift in frequency is negligible.

E. Parametric Analysis

The proposed metamaterial THz sensor is analyzed for certain design parameters such as the length of the hexagon arm (L3), the length of the conductor connecting the spin to the outer hexagon (L2), and the width of the arrow in the spin (d). The impact of the conductor length connecting the spin to the outer hexagon (L2) is optimized to 4.76 μm for better absorption characteristics as shown in Fig. 7a. The length of the connector is fixed to 4.76 μm which ends up with the hexagon. If the connector length is reduced to 4.56 μm and 4.36 μm, the width of the absorption characteristics is reduced which impacts the Full-Width Half Maximum (FWHM) but the resonant frequency remains the same. The impact of the length of the hexagon arm (L3) is analyzed and presented in Fig. 7b. It is inferred that the L3 value is optimized to 5.5 μm for the desired absorption characteristics. As the length of the hexagon arm decreases, the resonant frequency redshifts by 200GHz along with a second peak at a higher frequency. Similarly, the increase in the length of the hexagon arm, blueshifts the resonant frequency by 100 GHz with the same absorptivity as shown in Fig. 7b. Furthermore, the width of the arrow (d) in the spin is analyzed for different values and the corresponding absorption characteristic is depicted in Fig. 7c. The width (d) is optimized to 4.86 μm for obtaining desired absorption characteristics as shown in Fig. 7c. The increase in width (d), redshifts the absorption curve by 200 GHz whereas the decrease in d value results in blue shifts by 460 GHz.

III. Stability Analysis

The polarization stability is an important factor in the design of the THz sensor. If the polarization stability is considered, the effect of errors during the experiment can be ignored due to the improper placement of the sensor while multiple measurements are taken [32]. Thus, the polarization stability analysis is generated using the centrosymmetric structure. The proposed sensor is analyzed and reported in this section. The THz radiation is applied along the ‘z’ direction for the excitation of the proposed sensor. The normal incidence of THz radiation i.e., $\theta = 0^{o}$ is used to examine the TE (Transverse Electric) mode with $\phi = 0^{o}$ and TM (Transverse Magnetic) mode with $\phi = 90^{o}$. In the proposed structure, due to the symmetrical geometry, an identical characteristic of absorption for TE and TM mode is shown in Fig. 8.

Figure 9 depicts the response of the sensor on absorptivity for different oblique incidences of THz waves. The incident angle (θ) varies from 0° to 60° to measure the angular stability of the sensor. The sensor shows an identical characteristic for different angles. However, the increase in angle (θ), blueshifts the resonant frequency with an average deviation in frequency is less than 0.24% and absorptivity of 99.9%. Thus, the designed spin-shaped THz sensor is angularly stable upto the incidence angle of 60^{o}. Thus, it is

summarized from Fig. 8 and Fig. 9 that the designed THz sensor exhibits polarization and angular stability.

IV. Sensitivity Estimation

In this section, the sensitivity of the THz sensor is estimated from its sensing performance for analytes with different indexes of refractive profiles, and the results are presented. The sensing performance of the sensor is estimated using the analyte whose thickness, 'ta' is placed above the conducting layer as shown in Fig. 10. The different filler materials such as minerals, diatomaceous earth and talc are considered analytes in this research. These fillers when added with the polymers will reduce the cost of the materials [33]. The analyte is varied based on their unique refractive index value which varies from n = 1(air) to n = 2.67 (lead oxide). The dielectric constant ($_r$) is computed from the refractive index (n) which is known in prior. The thickness of the analyte, ta is fixed to be 1 μm.

The absorption characteristics of the designed metamaterial THz sensor for various refractive indices are depicted in Fig. 11. It is inferred that the increase in refractive index causes a redshift in the resonant frequency. The perturbation theory and the equivalent medium theory [32] are used in computing this redshift in frequency. The shift in resonant frequency is estimated using the fields in the sensor with respect to the change in dielectric constant using the Eq. (3).

$$\frac{\Delta\omega}{\omega_0} = \frac{-\int_{v_0}\left(\Delta\varepsilon\left|\bar{E}_0\right|^2 + \Delta\mu\left|\bar{H}_0\right|^2\right)dv}{\int_{v_0}\left(\varepsilon\left|\bar{E}_0\right|^2 + \mu\left|\bar{H}_0\right|^2\right)dv} = \frac{-\int_{v_0}\left(\Delta\varepsilon\left|\bar{E}_0\right|^2\right)dv}{\int_{v_0}\left(\varepsilon\left|\bar{E}_0\right|^2\right)dv} \quad (3)$$

where E_0 and H_0 are the electric and magnetic field in the sensor without analyte respectively, Δ and Δμ are the change in permittivity and permeability respectively. The equivalent medium theory is used to estimate the effective dielectric constant when the sensor is loaded by Eq. (4) [32].

$$_{eff} = _{sub} + \alpha\ _{air} + (1-\alpha)\ _r \quad (4)$$

The sensor performance is estimated using three different parameters viz. sensitivity (S), quality (Q) factor, and FWHM. Sensitivity is defined as the ratio of change in frequency (Δf) to the change in refractive index (Δn). Thus, the average sensitivity is estimated to be 1.37 THz/Refractive Index Unit (RIU) for refractive indices considered between n = 1 to n = 2.67. The absorptivity of 99.9% is also maintained for all the refractive indices up to 2.67 as shown in Table II. It is observed that the proposed sensor is highly sensitive for n = 1.41 with the sensitivity of 1.47 THz/RIU, whereas the THz sensor shows the least sensitivity for n = 2.67 with the sensitivity of 1.30 THz/RIU. The other parameters such as FWHM and Q factor are estimated and tabulated in Table II. Q factor is defined as the ratio of resonant frequency (fr) to

FWHM. The Q factor of 4.47 is obtained for the refractive index n = 1. From the table, it is inferred that, as the refractive index increases, the Q factor is reduced. The capacitance of the sensor estimates the Q factor. However, when the sensor is loaded with the analyte, the capacitance of the sensor is said to be an effective capacitance (C_{eff}). Thus, the effective capacitance is the total sum of the capacitance due to the sensor and the analyte (C_{sensor}) [12]. The capacitance of the sensor C_{sensor} is varied based on the change in the refractive index of the analyte, Therefore, the C_{eff} of the sensor varies. Thus, the quality factor of the THz sensor is affected due to the change in effective capacitance using the expression $Q = 1/\omega CR$. Hence, the Q factor and the capacitance of the sensor are inversely proportional to each other. Therefore, the increase in the refractive index of the load increases the effective capacitance in turn reduces the Q factor, and thus, the resonant frequency of the THz sensor is reduced.

TABLE II CHARACTERISTICS OF ABSORPTION FOR DIFFERENT REFRACTIVE INDEX PROFILE

RI	A (%)	S (THz/RIU)	Δf (THz)	FWHM (THz)	Q
1	99.9	-	-	1.6	4.47
1.41	99.7	1.47	0.60	1.65	3.97
1.73	99.9	1.37	1.00	1.55	3.97
2.00	99.3	1.36	1.36	1.6	3.67
2.23	99.5	1.46	1.65	1.5	3.67
2.44	99.6	1.33	1.92	1.5	3.49
2.67	98.6	1.30	2.14	1.35	3.71

Furthermore, the sensor performance for different thicknesses of the sample is analyzed and plotted in Fig. 12. The sample thickness is varied from 1 μm to 10 μm with a fixed refractive index n = 1.41. It is inferred from the figure that, as the thickness of the sample increases, the redshift in the frequency of 0.1 THz. Thus, the variation in the thickness of the analyte shows the average deviation of 59 GHz/μm. Similarly, the increase in thickness of the analyte reduces the absorptivity to 96%. The best curve fit is found using the R^2 value. The dependent variable (S) and independent variable (n) are related using the value of R^2. The value of R^2 is estimated for the linear curve is 0.9995 whereas, for the exponential fit, the R^2 value is 0.8719. Therefore, the linear curve fit is expressed using the equation S = 1.2644n-1.1747 (as shown in Fig. 13), where n is the refractive index of the analyte and S is the sensitivity of the sensor in THz/RIU.

The performance of other refractive index-based THz sensors reported in the literature is compared with the proposed THz sensor, which is presented in Table III. It is inferred from the table, that the proposed THz sensor is miniaturized compared to the works presented in the literature [15–17] by 23%, 76%, and 74% respectively. The proposed THz sensor exhibits high sensitivity compared to the references [13], [15–

17]. The estimated sensitivity is 56% greater than the sensitivity in the reference [13], compensating with the effective size of the sensor which is larger by 65%.

TABLE III COMPARISON OF PROPOSED SENSOR PERFORMANCE WITH OTHER RELEVANT WORKS

Ref.	Effective size ($\lambda_{eff} \times \lambda_{eff}$)	Geometrical Size (μm x μm)	% Miniaturization (refer λ_{eff})	*f* (THz)	Sensitivity (GHz/RIU)
[13]	0.391 × 0.391	36 × 36	-	2.249	300
[15]	0.763 × 0.763	140 × 140	23	1.52	430
[16]	1.368 × 1.368	500 × 500	76	0.557	128
[17]	1.317 × 1.317	300 × 300	74	0.22, 0.48, 0.72, 0.76	139.2
This work	**0.67 × 0.67**	**15 × 15**	**-**	**7.16**	**1370**

The following are the important features of the designed highly sensitive THz sensor:

1. The effective footprint of the proposed metamaterial THz sensor is 0.67 λ_{eff} x 0.67 λ_{eff} which is lesser by 23%, 76%, and 74% of the structures proposed in [15–17] respectively. Thus, the proposed design is ultra-miniaturized.

2. Maximum absorption of 99.9% is obtained at 7.16 THz in a free space environment.

3. A high sensitivity of 1.47 THz/RIU for the refractive index of 1.41 at 7.16 THz is offered by the proposed THz sensor, which is highest by 612% on average when compared to the works proposed in [13], [15–17].

4. It offers insensitive polarization characteristics and stable angular characteristics with less than 0.24% deviation upto the incident angle of 60˚.

5. The increase in thickness of the analyte is also analyzed and the average deviation of 59 GHz/μm is observed.

V. Conclusion

This work describes the design, characterization and analysis of THz sensor for material sensing application. The proposed metamaterial sensor is designed using a spin-shaped resonator within a hexagonal loop. The TE and TM polarization for the sensor is analyzed and inferred that the sensor is insensitive to the polarization. Further, the angular stability characteristics are analyzed for angles upto 60º without any loss in absorptivity and an average deviation of less than 0.24% is obtained. Later, the

performance of the sensor on sensitivity is analyzed and estimated for various analytes with their unique refractive indices. The highest sensitivity of 1.47 THz/RIU is offered by the sensor for the refractive index of 1.41. Similarly, the analyte thickness is analyzed for various values and the estimated deviation is 59 GHz/μm. Thus, it is concluded that an ultra-miniaturized THz sensor is proposed along with high sensitivity for various material sensing applications.

Declarations

Funding: This project did not receive any funding.

Conflicts of interest/Competing interests: The authors declare that there is no conflict of interest/competing interests.

Availability of data and material (data transparency): No new data generated and hence it is not applicable.

Code availability (software application or custom code): The work does not involve a computer code.

Additional declarations for articles in life science journals that report the results of studies involving humans and/or animals

Ethics approval: No human or animal subject is involved in the study. Hence not applicable.

Consent to participate: Not applicable.

Consent for publication: Not applicable.

References

1. Jornet, J.M., Akyildiz, I.F.: Graphene-based plasmonic nanoantenna for terahertz band communication in nanonetworks. IEEE J. Sel. Areas Commun. **31**(12), 685–694 (2013) “,”,
2. Jepsen, P.U., Cooke, D.G., Koch, M.: Terahertz spectroscopy and imaging—Modern techniques and applications. Laser Photon. Rev. **5**(1), 124–166 (2011) “,”,
3. Watts, C.M., Shrekenhamer, D., Montoya, J., Lipworth, G., Hunt, J., Sleasman, T., Krishna, S., Smith, D.R., Padilla, W.J.: Terahertz compressive imaging with metamaterial spatial light modulators. Nat. Photonics **8**(8), 605 (2014) “”, ,
4. Cong, L., Singh, R.: “Sensing with THz metamaterial absorbers”. arXiv preprint arXiv:,1408.3711, 2014
5. Wang, Z., et al.: "Characterization of Thin Metal Films Using Terahertz Spectroscopy". IEEE Trans. Terahertz Sci. Technol. **8**(2), 161–164 (2018)
6. Smith, D.R., Padilla, W.J., Vier, D.C., Nemat-Nasser, S.C., Schultz, S.: Composite medium with simultaneously negative permeability and permittivity. Phys. Rev. Lett. **84**(18), 4184 (2020) “”, ,

7. Viktor, G.: The electrodynamics of substances with simultaneously negative values of and μ. Sov Phys. Usp **10**, 509 (1968) “,” .
8. Ahmed, S., Sungjoon, L.: Recent advances in the metamaterial-inspired biosensors. Biosens. Bioelectron. **117**, 398–402 (2018) “,”,
9. Landy, N.I., Sajuyigbe, S., Mock, J.J., Smith, D.R., Padilla, W.J., Absorber, P.M.: Phys. Rev. Lett. **100**, 207402 (2008)
10. Butler, L., Wilbert, D.S., Baughman, W., Balci, S., Kung, P., Kim, S.M., "Design, simulation, and characterization of THz metamaterial absorber," 2011 International Semiconductor Device Research Symposium (ISDRS), College Park, MD, 2011, pp. 1–2
11. Wilbert, D.S., Hokmabadi, M.P., Kung, P., Kim, S.M., "Equivalent-Circuit Interpretation of the Polarization Insensitive Performance of THz Metamaterial Absorbers," in IEEE Transactions on Terahertz Science and Technology, vol. 3, no. 6, pp. 846–850, Nov. 2013
12. Ma, Anchen, et al., "Ultrasensitive THz Sensor Based on Centrosymmetric F-Shaped Metamaterial Resonators," Frontiers in Physics, pp. 441, 2020
13. Tao, A.S., Saadeldin, M.F.O., Hameed, E.M.A., Elkaramany, Obayya, S.S.A.: "Highly Sensitive Terahertz Metamaterial Sensor," in IEEE Sensors Journal **19**(18), 7993–7999 (2019)
14. Al-Naib, H., Ibraheem, R., Erik, Carsten, L., F. & Christodoulides, O., Demetrios, M., Tsuneyuki, R.: Conductive Coupling of Split Ring Resonators: A Path to THz Metamaterials with Ultrasharp Resonances. Phys. Rev. Lett. **112**, 183903 (2014) “”,
15. Reinhard, B., Schmitt, K.M., Wollrab, V., Neu, J., Beigang, R., Rahm, M.: Metamaterial near-field sensor for deep-subwavelength thickness measurements and sensitive refractometry in the terahertz frequency range. Appl. Phys. Lett. **100**(22), 221101 (2012) “,”,
16. Yahiaoui, R., Strikwerda, A.C., Jepsen, P.U.: "Terahertz Plasmonic Structure with Enhanced Sensing Capabilities". IEEE Sens. J. **16**(8), 2484–2488 (2016)
17. Yahiaoui, R., Tan, S., Cong, L., Singh, R., Yan, F., Zhang, W.: Multispectral terahertz sensing with highly flexible ultrathin metamaterial absorber. J. Appl. Phys. **118**, 083103 (2015)
18. Bai, J., Shen, W., Wang, S., et al.: An ultra-thin multiband terahertz metamaterial absorber and sensing applications. Opt. Quant. Electron. **53**, 506 (2021) “.”
19. Veeraselvam, A., Mohammed, G.N., Savarimuthu, K., et al.: A novel multi-band biomedical sensor for THz regime. Opt. Quant. Electron. **53**, 354 (2021) “.”
20. Tao, H., Bingham, C.M., Strikwerda, A.C., Pilon, D., Shrekenhamer, D., Landy, N.I., Fan, K., Zhang, X., Padilla, W.J., Averitt, R.D., “Highly flexible wide angle of incidence terahertz metamaterial absorber: Design, fabrication, and characterization”. physical review B, vol. 78, no. 24, pp.241103, 2008
21. Kandammathe Valiyaveedu, S., Mahalakshmi, P., Han, S., Vigneswaran, D., Mani, M.S., Rajan: Rajan Jha, and Ranjan Singh, "A terahertz Brewster switch based on superconductor hyperbolic metamaterial". J. Appl. Phys. **128**, 173106 (2020)

22. Padhy, P., Sahu, P., Jha, K.: R, “Metal Wire Waveguide Based All Plasmonic Refractive Index Sensor For Terahertz Frequencies”, Sensors and Actuators B: Chemical, 2015
23. Ding, P., Liang, E., Cai, G., Hu, W., Fan, C., Xue, Q.: Dual-band perfect absorption and field enhancement by interaction between localized and propagating surface plasmons in optical metamaterials. J. Opt. **13**, 075005 (2011) “
24. Kumar., S., Guo, Z., Singh, R., Wang, Q., Zhang, B., Cheng, S., Liu, F.Z., Marques, C., Kaushik, B.K., Jha, R.: "MoS2 Functionalized Multicore Fiber Probes for Selective Detection of Shigella Bacteria Based on Localized Plasmon". J. Lightwave Technol. **39**(12), 4069–4081 (2021)
25. Cai, S., Pan, H., González-Vila, Á, Guo, T., Gillan, D., Wattiez, R., Caucheteur, C.: Selective detection of cadmium ions using plasmonic optical fiber gratings functionalized with bacteria. Opt. Express **28**, 19740–19749 (2020)
26. Shchegolkov, D.Yu., Azad, A.K., O’Hara, J.F., Simakov, E.I.: "Perfect subwavelength fishnet like metamaterial-based film terahertz absorbers" Phys. Rev. B 82, 205117
27. Gelmont, B., Parthasarathy, R., Globus, T., Bykhovski, A., Swami, N.: "Terahertz (THz) Electromagnetic Field Enhancement in Periodic Subwavelength Structures". IEEE Sens. J. **8**(6), 791–796 (June 2008). doi:10.1109/JSEN.2008.923222
28. Yan, F., et al.: "Ultrasensitive Tunable Terahertz Sensor With Graphene Plasmonic Grating". J. Lightwave Technol. **37**(4), 1103–1112 (2019) 15 Feb.15
29. Barnes, W.L., Dereux, A., Ebbesen, T.W.: Surface plasmon subwavelength optics. Nature **424**(6950), 824–830 (2003) “,”,
30. Zhou, X., Zhang, T., Chen, L., Hong, W., Li, X.: A graphene-based hybrid plasmonic waveguide with ultra-deep subwavelength confinement. J. Light wave Technol **32**(21), 4199–4203 (2014) Nov. 1„ “,”,
31. Chamanzar, M., Soltani, M., Momeni, B., Yegnanarayanan, S., Adibi, A.: Hybrid photonic surface-plasmon-polariton ring resonators for sensing applications. Appl. Phys. B **101**(1), 263–271 (2010) “,”,
32. Tao, C., et al.: Design of a terahertz metamaterial sensor based on split ring resonator nested square ring resonator. Mater. Res. Express **7**, 095802 (2020) “”, ,
33. Wypych, G., “Physical Properties of Fillers and Filled Materials,” Handbook of Fillers, pp. 303–357, 5th edition, 2021

Figures

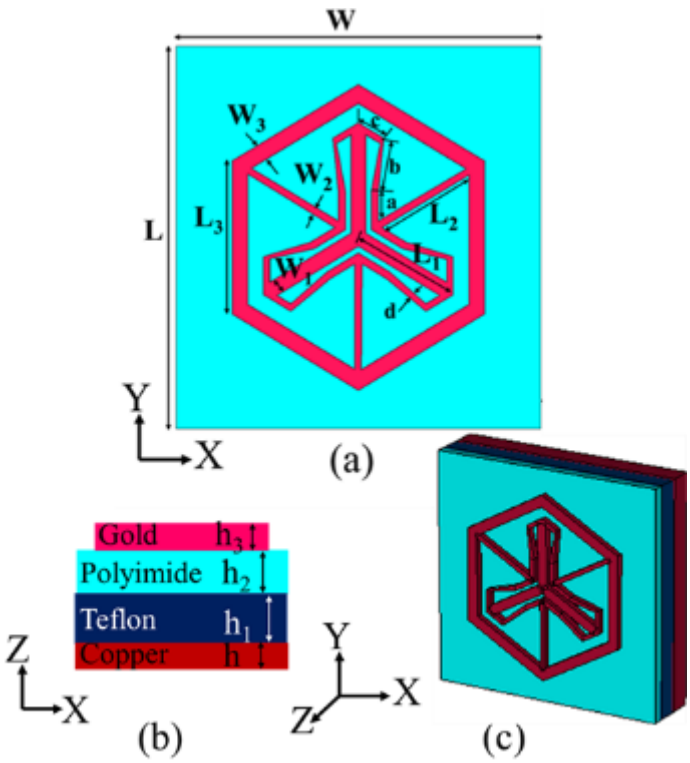

Figure 1

Proposed structure of the THz sensor in different views such as (a) Top (b) Side (c) Perspective

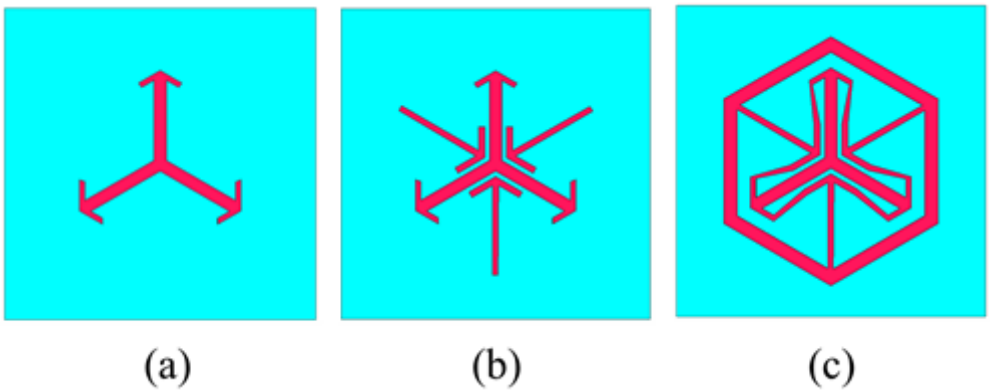

Figure 2

Development of the proposed structure (a) Absorber 1 (b) Absorber 2 (c) Proposed Absorber

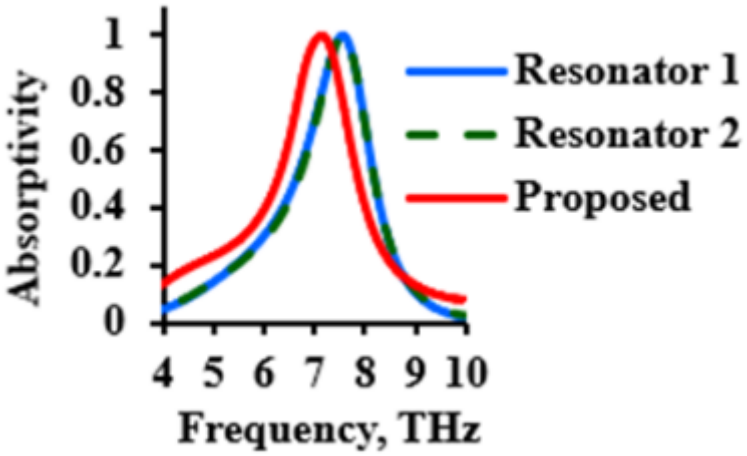

Figure 3

Characteristics of absorption at different stages of development.

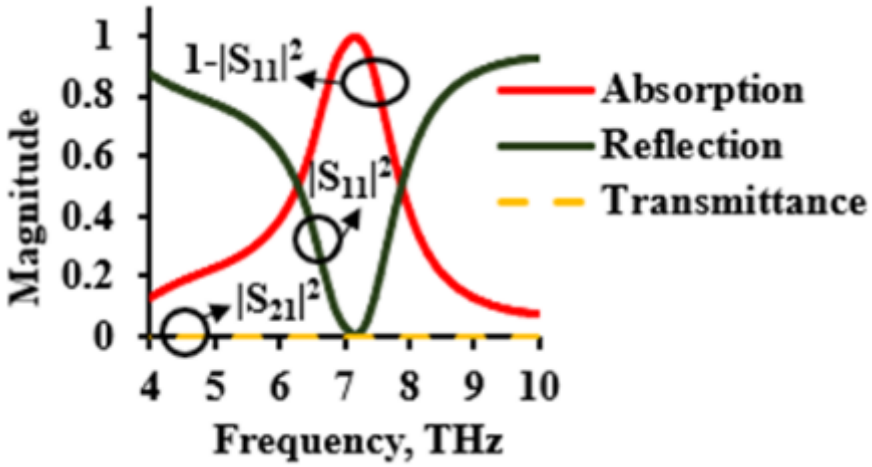

Figure 4

Characteristics curves for transmittance, absorption, and reflection of the metamaterial THz sensor

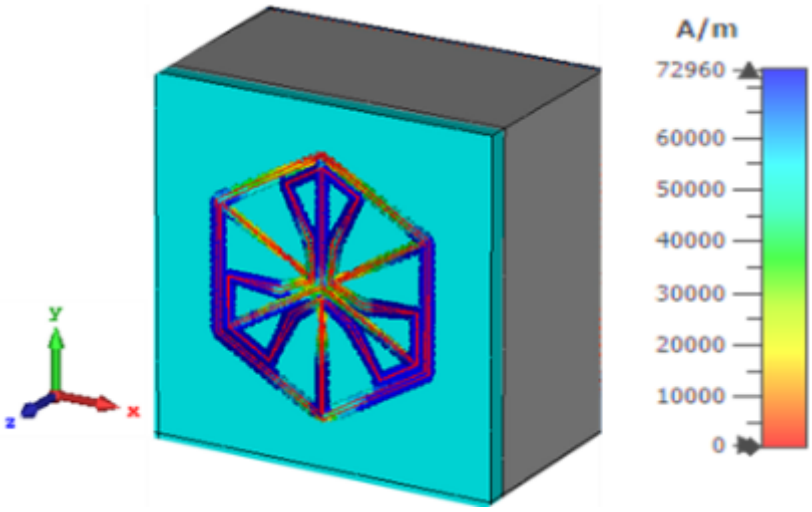

Figure 5

Surface plasmon density at 7.16 THz for the proposed THz sensor

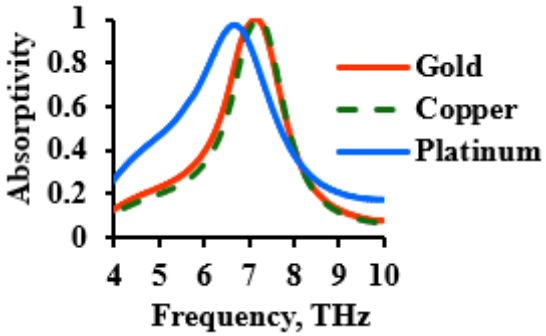

Figure 6

Absorption characteristics for various conductors in THz sensor

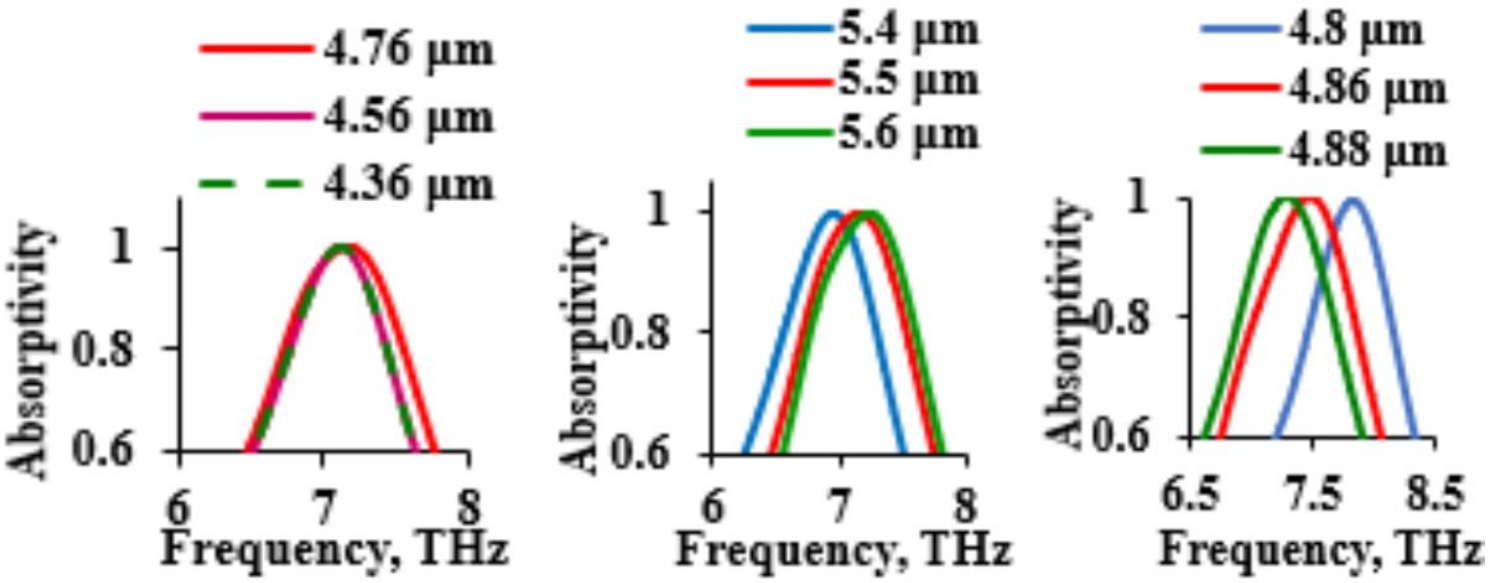

Figure 7

The influence of the parameters like (a) conductor length (L2), (b) the length of the hexagon arm (L3), and (c) the width (d) of the spin, on the characteristics of absorption.

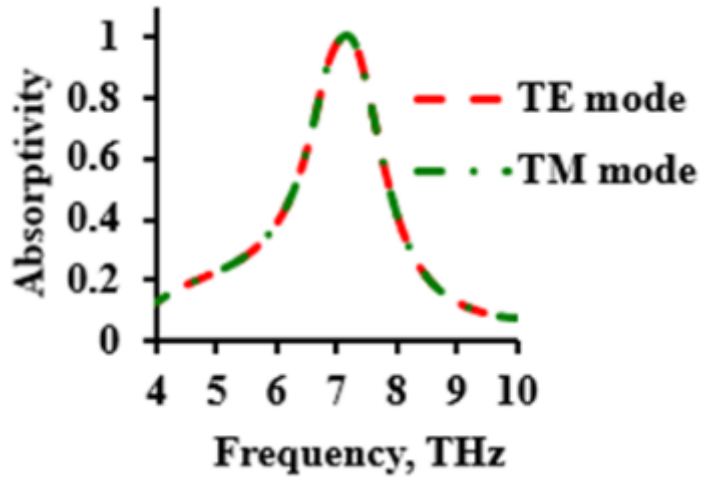

Figure 8

Polarization stability characteristics of the proposed sensor

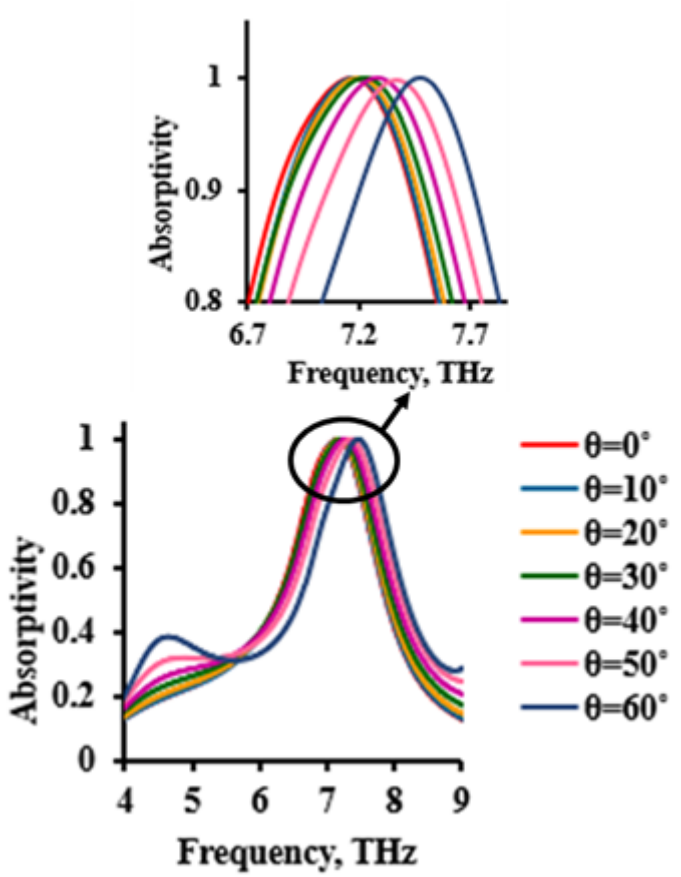

Figure 9

Angular stability characteristics of the proposed sensor

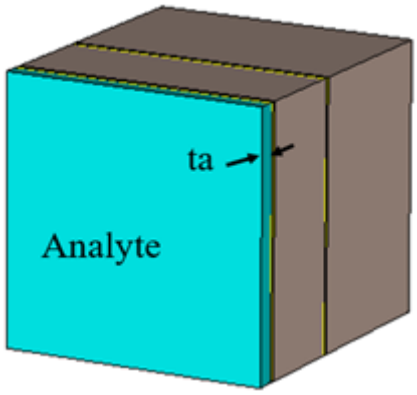

Figure 10

Experimental setup for sensitivity estimation

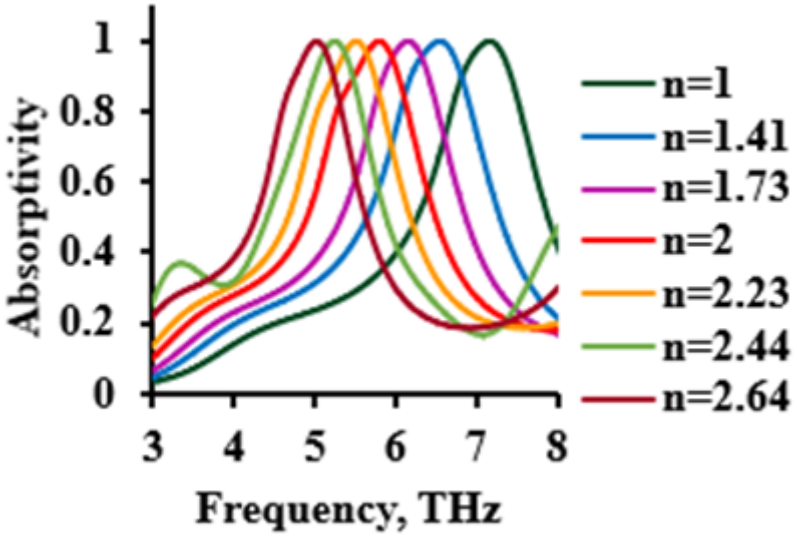

Figure 11

Absorption characteristics for different values of refractive index

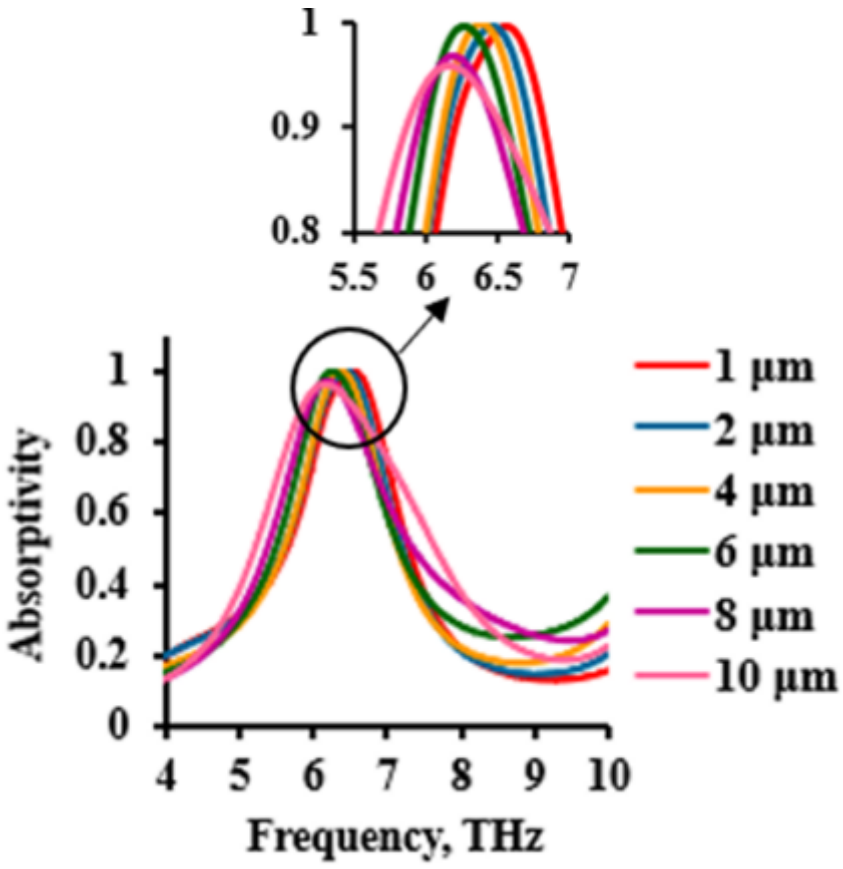

Figure 12

Performance of the sensor for different analyte thicknesses

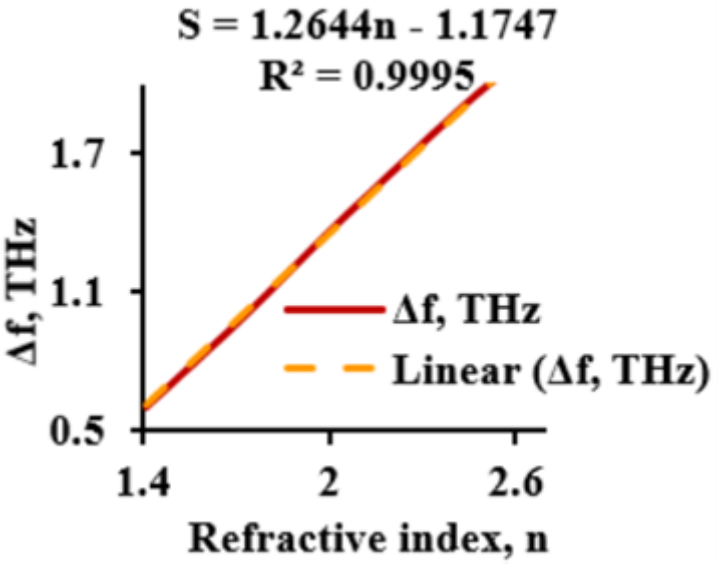

Figure 13

The linear curve fit for sensitivities by varying the refractive indices